Geofísica internacional
ISSN: 0016-7169
Universidad Nacional Autónoma de México, Instituto de Geofísica

Darawcheh, Ryad; Ghazzi, Riad Al; Abdul-Wahed, Mohamad Khir

Empirical relationship for assessing the near-field horizontal coseismic displacement using GPS Seismology data

Geofísica internacional, vol. 60, no. 1, 2021, January-March, pp. 31-50
Universidad Nacional Autónoma de México, Instituto de Geofísica

DOI: https://doi.org/10.22201/igeof.00167169p.2021.60.1.2025

Available in: https://www.redalyc.org/articulo.oa?id=56871788003

Original paper

Empirical relationship for assessing the near-field horizontal coseismic displacement using GPS Seismology data

Ryad Darawcheh [1, 2 *], Riad Al Ghazzi [3] and Mohamad Khir Abdul-Wahed [2]

Received: December 29, 2019; accepted: October 26, 2020; published online: January 1, 2021

Resumen

En esta investigación se reunió un conjunto de datos de desplazamiento cosísmico GPS horizontal en el campo cercano en todo el mundo, con el propósito de investigar una posible relación entre el desplazamiento cosísmico GPS y los parámetros del terremoto. Se Se aplicó un análisis de regresión a los datos de 120 terremotos interplaca con magnitud (Mw 4,8-9,2). Se encontró una relación empírica preliminar para la predicción del desplazamiento cosísmico GPS horizontal de campo cercano en función de la magnitud del momento y la distancia entre el hipocentro y la estación GPS de campo cercano utilizando el análisis de regresión múltiple. La relación obtenida se ha aplicado preliminarmente para evaluar los desplazamientos cosísmicos asociados con algunos grandes terremotos históricos ocurridos a lo largo del sistema de fallas del Mar Muerto. Esta relación global podría ser útil en todo el mundo para evaluar el desplazamiento cosísmico en cualquier punto alrededor de las fallas activas.

Palabras clave: desplazamiento cosísmico, sismología con GPS, análisis de multi regresión, sistemas de fallas del Mar Muerto.

Abstract

In this research, a data set of horizontal GPS coseismic displacement in the near-field has been assembled around the world to investigate a potential relationship between the GPS coseismic displacement and the earthquake parameters. Regression analyses have been applied to the data of 120 interplate earthquakes with magnitude (M_w 4.8-9.2). A preliminary empirical relationship for prediction near-field horizontal GPS coseismic displacement as a function of moment magnitude and the distance between hypocenter and near field GPS station has been established using the multi regression analysis. The obtained relationship has been preliminarily applied to assessing the coseismic displacements associated with some large historical earthquakes occurred along the Dead Sea fault system. Such a global relationship could be worldwide useful for assessing the coseismic displacement at any point around the active faults.

Key words: GPS coseismic displacement, GPS seismology, multi regression analysis, Dead Sea fault system.

**Corresponding author: rdarawcheh@aec.org.sy*

1 Syrian Virtual University, Damascus, P.O. Box 35329, Syria

2 Department of Geology, Atomic Energy Commission of Syria, Damascus, Syria

3 Syrian Private University, Damascus, Syria

INTRODUCTION

Global Positioning System (GPS) technology has been widely used for more than 25 years for measuring crustal coseismic displacement due to earthquakes, which is so-called GPS Seismology. In fact, the first earthquake, whose displacement was measured by GPS, is the Loma Prieta (California) earthquake with moment magnitude (M_w 6.9) occurred in 1989 (Williams and Segall, 1996). After this earthquake, hundreds of papers have been published following the occurrence of moderate to large magnitude earthquakes. The GPS Seismology is also used along with other space and seismological tools (i.e. InSAR and strong motion) to understand the crustal deformation due to earthquakes. The coseismic displacement, derived by GPS, is of importance to seismic hazard assessment studies. It can support both the modeling of causative fault rupture and seismic moment (source parameters), as well as contributing to tsunami warning systems (e.g. Branzanti *et al.*, 2013). The magnitude and epicenter information is determined immediately after a destructive earthquake. However, the damage distribution is not a simple function of these two parameters alone. More detailed information, such as the horizontal coseismic displacement, is needed. Therefore, it is highly desirable to identify this displacement in the damaged area.

The aim of this work is to investigate a potential relationship between the horizontal GPS coseismic displacement and the earthquake parameters such as the magnitude. A data set of horizontal GPS coseismic displacement in the near-field has been collected around the world. The data is, then, processed by regression analyses to estimate the empirical relationship linking the near field horizontal GPS coseismic displacement as a function of other independent variables, such as the moment magnitude (M_w). This work can be directed to seismic hazard applications, especially in areas of a low level of instrumental seismic activity such as Syria, where the empirical relationship might be applied on data coming from a macroseismic analysis in the pre-instrumental period. In this perspective, the new empirical relationship could be helpful to predicate the coseismic displacements associated with the large historical earthquakes that occurred along the Dead Sea fault system (DSFS) along the northwestern plate boundary between the Arabian and Sinai plates. Furthermore, in most cases, where the GPS data are not available for all regions in the world, the empirical relations could be helpful in these regions. The importance of the work is that, to the best of our knowledge, there are no published works dealing with such a topic. Therefore, it could be the first attempt in this trend.

DATA AND METHODS

The derivation of the GPS coseismic displacements empirical relationship has been carried out through the three following steps. The first step is the data gathering and selection, whereas the worldwide GPS seismology data have been collected in the near-field of the earthquakes. The second step is the data analysis with the validation of the data set and the application of appropriate regression analysis to derive the target empirical relationship. The third step is a preliminary application of the derived empirical relationship for large historical and some instrumental earthquakes occurred along the DSFS.

In the first step, the data set has been selected according to the following criteria: 1) GPS station should be located in the near field and the epicentral distance less than 100 km; 2) Earthquake focus should be shallow and its depth less than 70 km; and 3) Moment magnitude should be moderate to large one. According to these selection criteria, 120 events occurred within the period from 1989 to 2017 have been selected. This data set includes mainly the GPS coseismic

displacements due to the interplate earthquakes. The data set is reviewed gradually to get the seismological and geodetic parameters and the necessary information for each earthquake. Recently, the GPS coseismic displacement database has been made available via so many websites and published in a lot of papers. Our data has been collected from 125 relevant papers and documented results at few related websites. The compiled database, selected according to the above criteria, includes for each event the earthquake parameters such as date, epicenter, focal depth (h) and moment magnitude (M_w), and the faulting type (normal, strike-slip and thrust). In addition, it includes the relevant GPS data such as the near-field GPS station code (ID), the distance between the epicenter and the nearest GPS station (Δ), near-field GPS coseismic horizontal displacement (D_{GPS}), type of measurement (e.g. survey GPS or continuous GPS). Appendix 1 lists the seismological-GPS parameters used in this study for 120 events within the period from 1989 to 2017. Note that GPS coseismic displacements were measured for the first time for the (M_w 6.9) Loma Prieta, California, earthquake in 1989. The last event in Appendix 1 is an earthquake of (M_w 6.6) that occurred in 2017 in the Aegean Sea between Turkey and Greece. Fig. 1 shows the distribution of the earthquakes listed in Appendix 1. We can observe that most of these earthquakes are distributed along the plate boundaries.

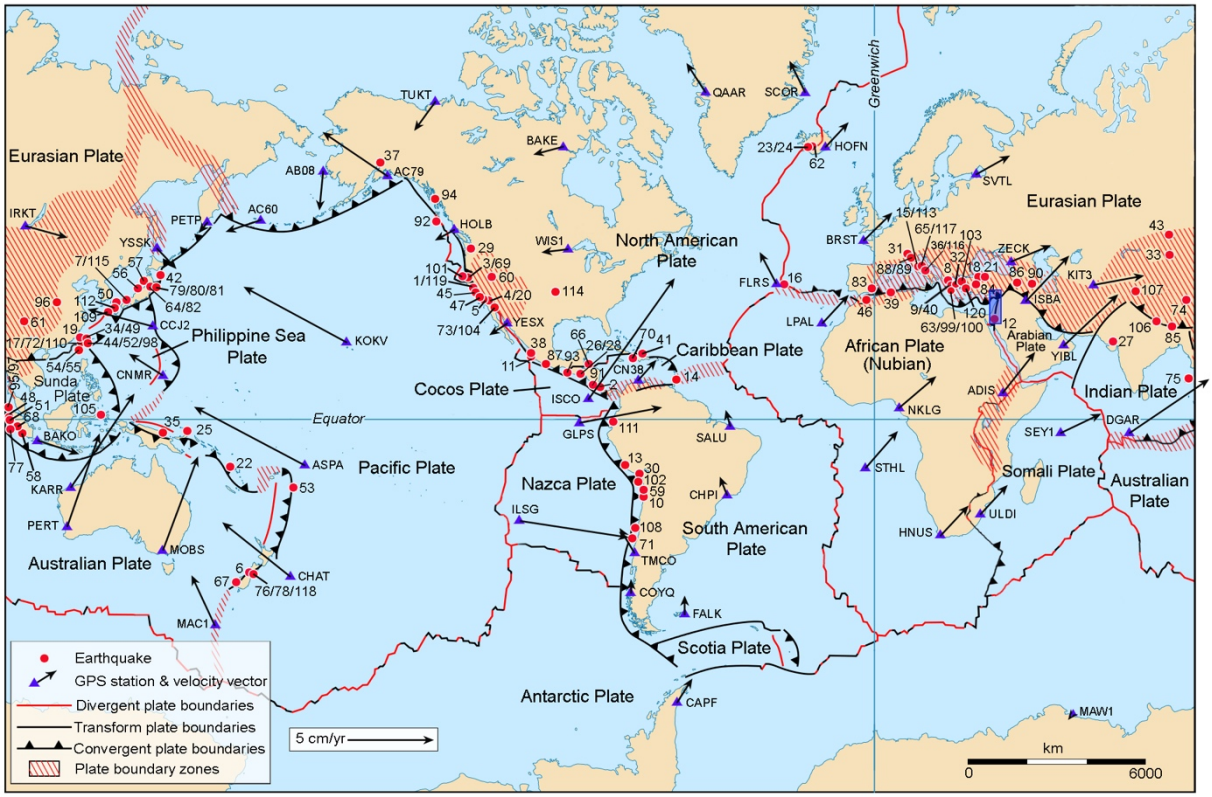

Figure 1. Simplified world map showing the spatial distribution of the 120 earthquakes occurred along the plate boundaries, listed in Appendix 1. The map shows locations of selected GPS stations and their velocity vectors to give an idea on the general directions of the tectonic plates. The rectangle is the location of the DSFS. GPS stations and its velocity vectors are plotted based on NASA database of present-day plate motions (Heflin, n.d.), according to the IGS08 reference frame and the reference ellipsoid of GRS80.

The data set has been adopted, where the seismological data includes many types of magnitude. In this regard, we have adopted the moment magnitude (M_w) since it is considered a more reliable measure of the energy released during an earthquake. Some earthquakes in our data set have surface wave magnitude. Since we have preferred (M_w), the surface wave magnitude (M_s) has been converted to (M_w) using the following empirical relation (Scordilis, 2006):

$$M_w = 0.67\ (\pm\ 0.005)\ M_s + 2.07\ (\pm\ 0.03) \quad (1)$$

The data sets are restricted to earthquakes with (M_w) greater than and equal to 4.8. Most coseismic displacements, shown in Appendix 1, are taken directly from published papers, while, in few cases, they have been calculated by the authors through the geometric sum of the 2 horizontal components (east-west and north-south). Although the coverage is not uniform neither time nor area due to availability of GPS seismology data in the near field, we believe that the data in Appendix 1 could be adequate for derivation a relationship between GPS coseismic displacement and magnitude and the hypocentral distance to the GPS stations.

In the second step, a preliminary statistical analysis for deriving the intended relationship has been performed using Microsoft Excel in order to estimate its general form. Professional statistical analysis is, then, applied using the Number Cruncher Statistical System (NCSS) in order to get an adequate relationship. The NCSS provides a multi regression analysis for studying the relationships among a dependent (Y) variable in the function of one or more independent (Xs) variables (NCSS, 2016). Regression analysis is one of the most important tools widely used in statistical modeling of the data, i.e. deriving the relationships among variables. It helps in understanding how a dependent variable changes when one or more independent variables are varied. The idea behind the derivation of the relationship has emerged from a general seismological-geodetic observation that is at a single near-field GPS station of any earthquake, the larger the earthquake magnitude, the bigger the GPS coseismic displacement. Therefore, we selected the GPS coseismic displacement (D_{GPS}) to be a dependent variable, and the moment magnitude (M_w) to be an independent variable. We also added, later on, the distance between the near-field GPS site and the earthquake hypocenter ($R_{hyp}= (\Delta^2+h^2)^{0.5}$) as a second independent variable. More details on the statistical processing have been presented in the next section.

Results

1 Derived Empirical Relationship

A preliminary analysis for estimation the general form of the target empirical relationship was performed using simple linear regression, provided by the "Microsoft Excel". It has indicated that there is no obvious linearity among (D_{GPS}) and (M_w). This result is confirmed by the weakness of the correlation coefficient (R^2=0.46). Another trial test was performed using the exponential regression, where the trending line is more compatible with the experimental points (Fig. 2) than whose of linear regression with a moderate correlation coefficient (R^2=0.52). The last estimated relationship is:

$$D_{GPS} = 0.0003\ e^{1.6242\ Mw} \quad (2)$$

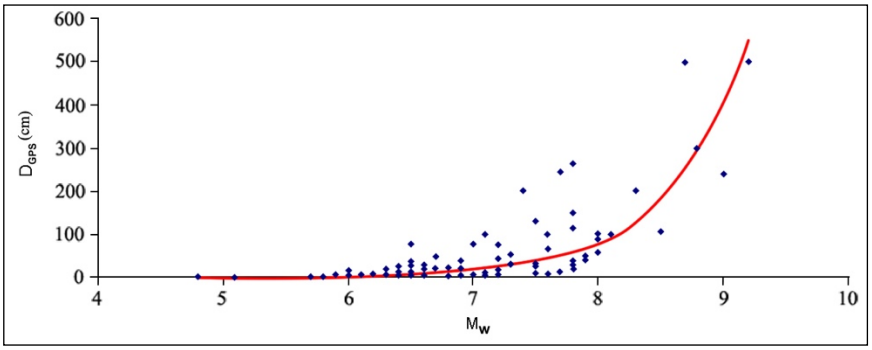

Figure 2. The empirical relationship estimated by the exponential regression.

Both previous correlation coefficients could be considered very low for establishing a reasonable empirical relationship. The reasons for the small level of the correlation coefficients could be interpreted by interfering other affecting factors or independent variables such as: 1) the hypocentral distance of earthquakes; 2) the effect of local geology "site effect" on the GPS displacement; 3) the faulting mechanisms; 4) the directivity effect due to the slip on the fault; 5) the differences of the ITRF used; 6) the differences between the processing software. Therefore, it is predicted that the target relationship will not be of a naive form and a simple regression will not be effective to give a reasonable correlation coefficient. A sophisticated form can be obtained using a multi regression analysis, where many affecting factors could be taken into consideration. In this case, the correlation coefficient could be close to 1.0. In this regard, an advanced professional program "Number Cruncher Statistical System (NCSS) (NCSS, 2016)" has been used for the improvement of our data set modeling. The exponential model should be modified to take the logarithms of the dependent variable (M_w). The relationship (2) becomes a simple linear regression (Figure 3):

$$\log D_{GPS} = -3.4943 + 0.6677\ M_w \quad (3)$$

with (R^2=0.52). This relationship is still inappropriate because of the moderate correlation coefficient. However, the last relationship needs more improvement using an advance analysis model and additional variables, such as the distance between the GPS station and the focus of the earthquake (R_{hyp}). A good solution has been obtained by multiple linear regression, which gives the optimum fit and results in the following relationship:

$$\log D_{GPS} = -4.8065 + 0.9269\ M_w - 0.0127\ R_{hyp} \quad (4)$$

with the correlation coefficient (R^2=0.66) and the root mean square of error (RMS=0.45) representing the uncertainty in ($\log D_{GPS}$). Thanks to the second independent variable, the relationship has been visibly improved. In the relationship (4), the (D_{GPS}) unit is cm and (R_{hyp}) is hypocenter–to- GPS station distance in km.

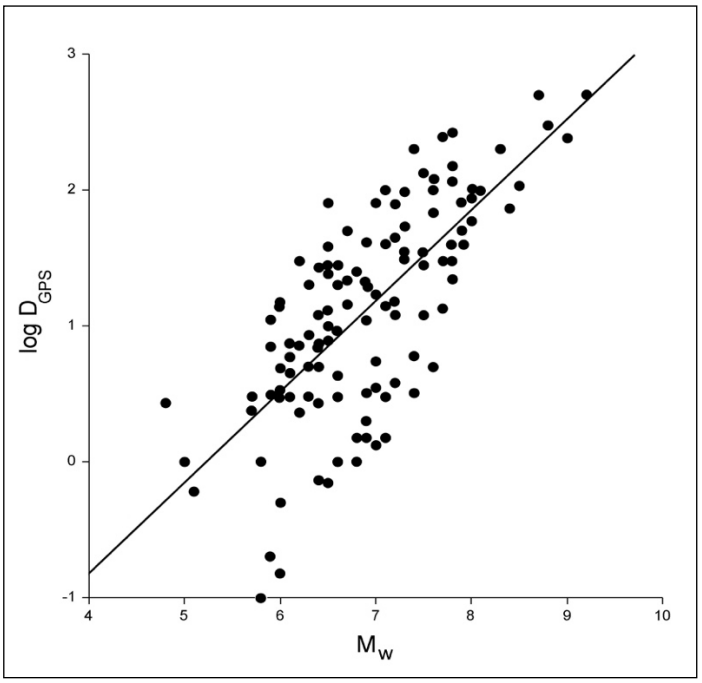

Figure 3. The empirical relationship estimated by taking the logarithm of relation (2).

In the NCSS, the regression problem has been solved by the least-squares method, where the regression coefficients are selected so as to minimize the sum of the squared residuals. The multiple regression analysis, applied in this research, has studied the relationship between a dependent variable (D_{GPS}) and two independent variables (M_w and R_{hyp}). In the relationship (4), the intercept (−4.8065) is the point at which the regression plane intersects the (log D_{GPS}) axis. The regression coefficients (0.9269 and – 0.0127) are the slopes of the regression plane in the direction of axis (M_w) and (R_{hyp}), respectively. These coefficients are called the partial-regression coefficients. Each partial regression coefficient represents the net effect of its variable on the dependent variable, holding the remaining independent variables in the equation constant. Once the regression coefficients have been estimated, various indices are studied to determine the reliability of these estimates. One of the most popular of these reliability indices is the correlation coefficient (R^2). The correlation coefficient is an index that ranges from -1 to 1. When the value is near zero, there is no linear relationship. As the correlation gets closer to plus or minus one, the relationship is stronger. A value of one (or negative one) indicates a perfect linear relationship between two variables. In the relationship (4), the correlation coefficient (R^2=0.66) indicates an acceptable linear relationship between the dependent variable (log D_{GPS}) and the two independent variables (M_w and R_{hyp}). In the regression analysis, the underlying assumptions include that the sample is representative of the population; the independent variables are measured with no errors. In fact, more than one variable may play an effective role in this idea.

The residual analysis is performed to evaluate the empirical equation, obtained from the regression analysis. The residuals can be graphically analyzed in numerous ways. Pertain to that, we examined three types of the residuals; they are the histogram, the normal probability plot, the scatter plot of the residuals versus the sequence of the observations. The histogram of the residuals is to evaluate whether they are normally distributed. On the histogram, shown in Figure 4, we can visually evaluate the normality of residuals. For visually evaluating normality of the

residuals, the better choice could be the normal probability plot (Figure 5), where the majority of data points are fallen along a straight line through the origin with a slope of 1.0. Some deviations from this straight line reflect departures from normality. Stragglers at either end of the normal probability plot indicate outliers, and the curvature at both ends of the plot indicates long or short distributional tails. In addition, a plot of the dependent variable (log D_{GPS}) versus the first independent variable (M_w), and versus the second independent variable (R_{hyp}) could be useful to show outliers (Figure 6).

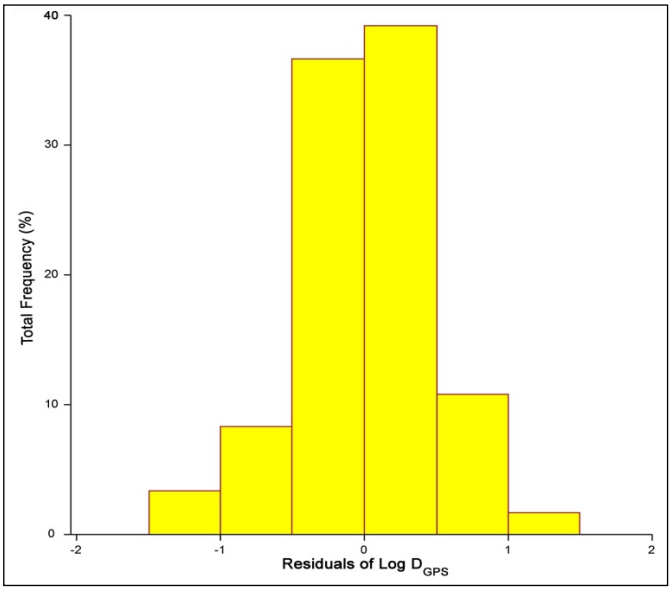

Figure 4. Histogram of the residuals distribution.

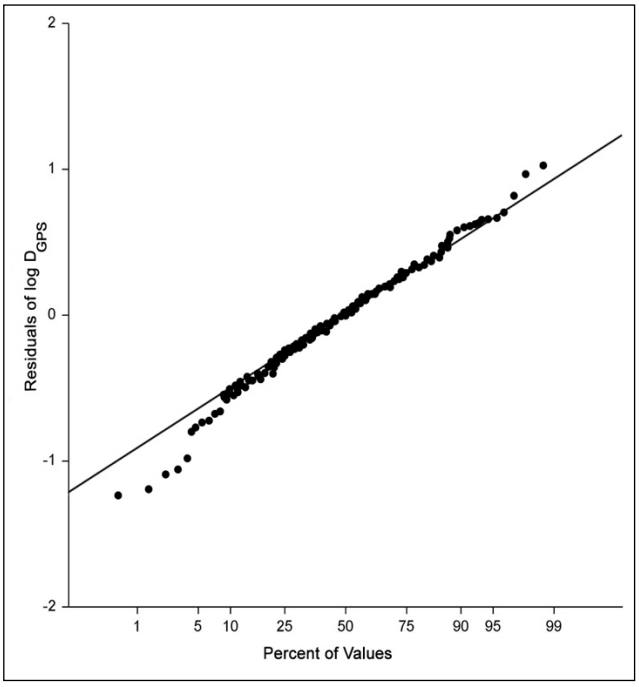

Figure 5. Normal probability plot of residuals.

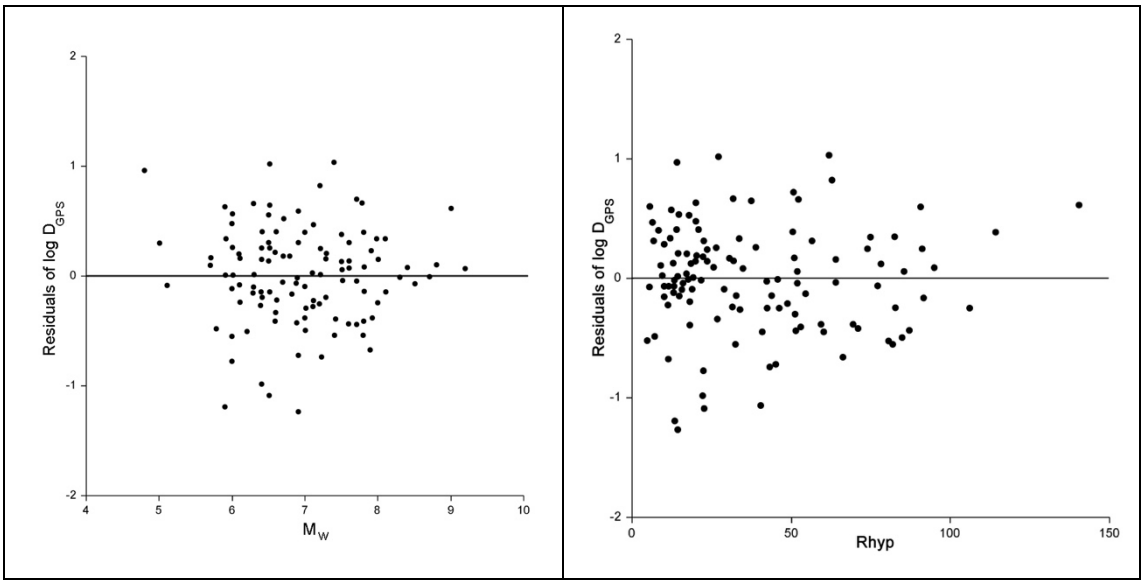

Figure 6. Left: A plot of (log D_{GPS}) versus (M_w). Right: A plot of (log D_{GPS}) versus (R_{hyp}).

2 Preliminary Application

The last step in this research is the preliminary application of the obtained empirical relationship (4) for some large earthquakes occurred along the DSFS. The recent instrumental seismicity of Syria has produced a little number of low magnitude events (Abdul-Wahed & Al-Tahan, 2010; Abdul-Wahed *et. al.*, 2011; Abdul-Wahed *et al.*, 2018). Therefore, no GPS Seismology data are available in the region even along the DSFS. However, several large well-documented historical earthquakes occurred along the DSFS (Table 1 and Figure 7). In this case, the obtained empirical relationship (4) could be helpful to estimate the coseismic displacement causing the historical earthquake destruction in Syria. The DSFS is a regional active left-lateral strike-slip fault system that runs for about 1000 km long from the Gulf of Aqaba in the south to the East Anatolian fault system (EAFS) in the north near Antakia. It forms a transform boundary between the Sinai plate (part of the larger African Plate) to the west and the Arabian plate to the east. Both plates are moving in a general north-northeast direction, but the Arabian plate is moving faster, resulting in the observed left lateral motion. A set of large historical earthquakes along the DSFS is shown in Figure 7 and listed in Table 1 with depth according to the published literature. The related magnitude (M_s) has been converted to moment magnitude (M_w) using the empirical relation (1). The horizontal coseismic displacements have been estimated using the relationship (4) at the epicenter, where $\Delta=0$. The results, shown in Table 1, demonstrate that the larger the earthquake magnitude, the bigger the GPS coseismic displacement. It could be useful to compare these empirical results with the real measurements of GPS stations. This comparison is enabled for an instrumental Nuweibaa earthquake, which occurred on 22 Nov. 1995 in Aqaba Gulf at the southernmost of the southern DSFS (Figure 7). The Dahab GPS station (DHAB) located at 26 km in the south-west of the epicenter, has documented a coseismic displacement of 17 cm (Kimata *et al.*, 1997). The empirical results, shown Table 1, demonstrate the estimated coseismic displacement to be 33.36 cm at the epicenter of Nuweibaa earthquake. Taking into consideration the epicentral distance to the Dahab GPS station, the relationship (4) yields to 20 cm as coseismic displacement. The difference between the observed displacement and the estimated one is about 3 cm, where the relative error is about 15%. Therefore, the empirical relationship (4), obtained

in the current research, could be fairly acceptable regarding the influence of numerous affecting factors.

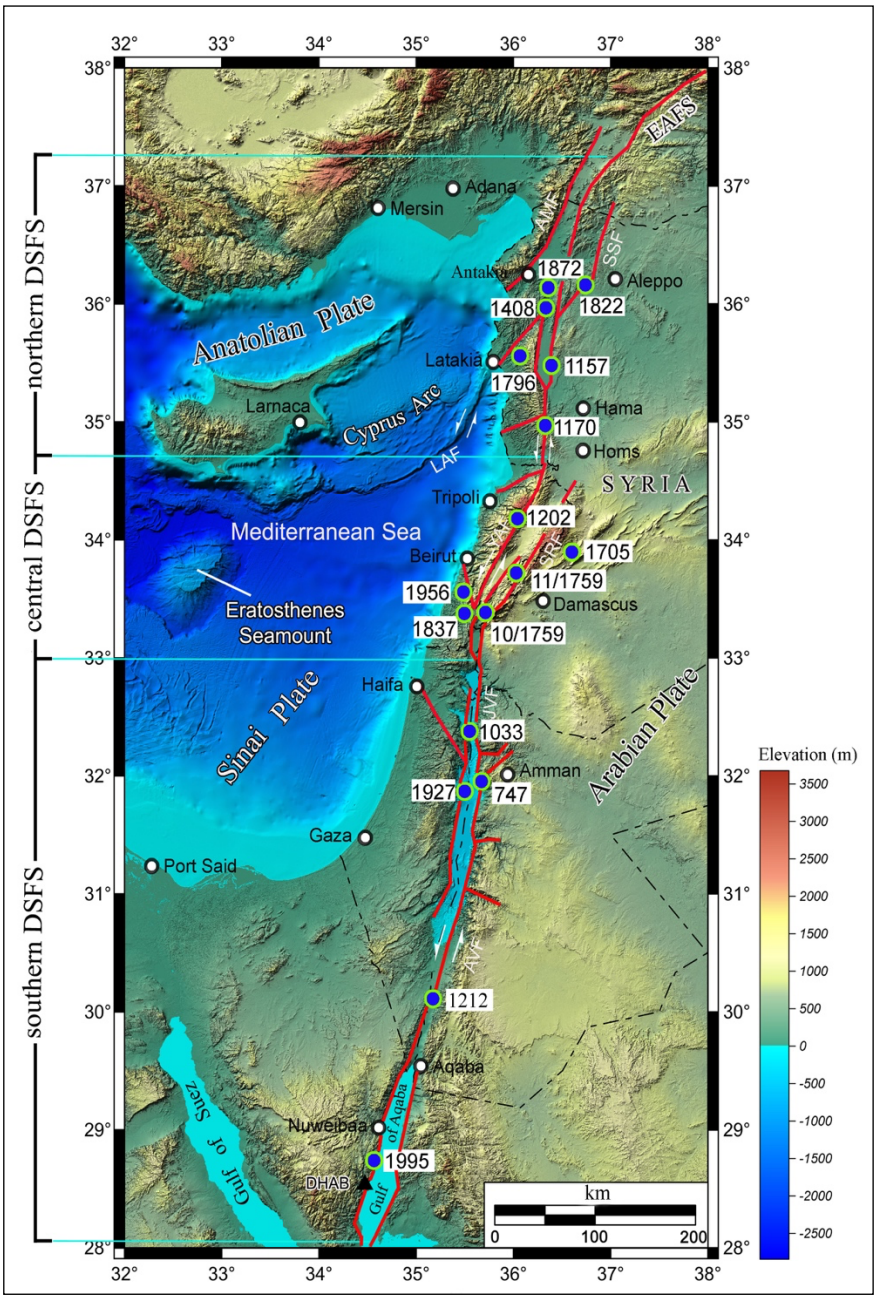

Figure 7. A digital elevation map of the easternmost Mediterranean showing distribution of the large historical earthquakes and some selected instrumental earthquakes (blue circles) occurred along the Dead Sea Fault system (red color line). Abbreviations of the active faults: AMF: Amanus fault; AVF: Araba Valley fault; EAFS: East Anatolian fault system; JVF: Jordan Valley fault; LAF: Latakia fault; SSF: Saint Simeon fault; SRF: Serghaya fault; YAF: Yammouneh fault. Topographic and bathymetric data are from the United States Geological Survey (USGS) and the European Marine Observation and Data Network (EMODnet), respectively. Black triangle is a location of GPS station named ad-Dahab (DHAB).

Table 1. A list of large historical earthquakes along with some selected instrumental earthquakes occurred along the DSFS. It includes the date of the earthquake, the locality of strongest effect, the references, the moment magnitude (M_w), the focal depth, and the estimated horizontal coseismic displacements (D_{GPS}).

Date	Earthquake	Reference(s)	M_w	R_{hyp} =h (km)	D_{GPS} (cm)
18 Jan. 747	Galilee	Sbeinati *et al.*, 2005; Ambraseys *et al.*, 1994	6.9	25	18.66
05 Dec. 1033	Jordan Valley	Ambraseys *et al.*, 1994	6.8	25	15.06
12 Aug. 1157	Hama	Sbeinati *et al.*, 2005	7.0	15	31.02
29 Jun. 1170	Missyaf	Sbeinati *et al.*, 2005	7.1	35	21.42
20 May 1202	Baalbak	Ambraseys and Melville, 1988	7.0	30	20.02
01 May 1212	Shaubak	Ambraseys *et al.*, 1994	6.8	25	15.06
29 Dec. 1408	Shughur	Sbeinati *et al.*, 2005; Ambraseys & Melville, 1995	7.0	25	23.17
24 Nov. 1705	Yabroud	Ambraseys & Finkel, 1993; Sbeinati *et al.*, 2005	6.6	35	07.37
30 Oct. 1759	Safad	Ambraseys and Barazangi, 1989	6.4	20	07.45
25 Nov. 1759	Damascus	Ambraseys and Barazangi, 1989	7.0	30	20.02
26 Apr. 1796	Latakia	Sbeinati *et al.*, 2005	6.4	20	07.45
13 Aug. 1822	Aleppo	Sbeinati *et al.*, 2005; Darawcheh *et al.*, 2019	7.0	18	28.42
01 Jan. 1837	W. Bekaa	Sbeinati *et al.*, 2005	7.0	20	26.81
03 Apr. 1872	Umeq	Sbeinati *et al.*, 2005	6.8	10	23.42
11 Jul. 1927	Nablus	Zohar and Marco, 2012	6.3	15	06.96
16 Mar. 1956	Chim	International Seismological Center	5.5	15	01.26
22 Nov. 1995	Nuweibaa	Al-Tarazi, 2000	7.0	12.5	33.36

DISCUSSION

The current study presents a synthesis of a large number of GPS measurements of near-field coseismic displacements associated with worldwide earthquakes during the modern period of GPS observations. The derived relationship relates the GPS coseismic displacement (as a dependent variable) to the moment magnitude and the distance between the GPS stations and the earthquake hypocenter (as independent variables). However, other factors or independent variables such as local geology (site effect), faulting mechanisms, and directivity effect due to the slip on the fault could affect this relationship. Unfortunately, these factors have not been included in the relationship. In fact, most of GPS stations are installed on rocky sites or bedrocks. In this case, the relationship is likely not affected by the site effect. However, the effect of faulting mechanisms and directivity merit to be studied and investigated in further works. In this study, surveying a wide range of GPS seismology dataset could make the established relationship global, and not confined for specific conditions. Consequently, this relationship could be a worldwide applicable.

Going back to the late 1960s, the relationship between near-field displacements and fault slip were beginning to be explored using simple kinematic models involving a dislocation in an elastic half-space. One of the earlier studies is Savage and Burford (1973) which applied this concept to the San Andreas fault using trilateration measurements. Such study examines the strain accumulation phase of the earthquake cycle – thus, the system is modeled as a fault that is slipping from surface to the base of the locking depth. This model (and more complicated ones) can be used to fit geodetic observations (GPS, InSAR, and classic terrestrial measurements) to estimate, by using the inverse solution, the near-field displacement in function of the fault slip rate and the position in the survey site. As one can see from the simple mathematical models, there is a predictable relationship between distance and local displacement for a given amount

of fault slip, which is directly related to earthquake moment and magnitude following well established relationships from instrumental data (e.g., Wells and Coppersmith, 1994). This relation also depends on the locking depth. Also, it is to mention that the locking depth can vary from one location to the next, even along the same fault (e.g., Smith-Konter *et al.*, 2011) which discussed the case of San Andreas fault. Therefore, the locking depth is not an easy task to be taken into consideration in the derived relationship (4). As regard with the DSFS, a variation in locking depth along the southern DSFS (Figure 7) has been observed from GPS measurements (Al-Tarazi *et al.*, 2011). It is important to realize that, in practice, there is considerable uncertainty and a range of values for locking depth estimates. Also, the locking depth for faults along the central DSFS (i.e., Yammuneh and Serghaya faults) are not well determined. Therefore, our globally estimated relationship could be preliminary and applicable with some caution.

CONCLUSION

In this study, an attempt was made to derive an empirical relationship for a preliminary assessment of coseismic horizontal displacement values in the near field. The dataset, compiled for this research, has served as a basis for empirically establishing a relationship of the GPS coseismic displacement as a function of the moment magnitude and the distance between the GPS stations and the earthquake hypocenter. The coseismic horizontal displacement values, recorded at 120 GPS stations from 120 different earthquakes around the world of moment magnitude greater than 4.8, have been used for the regression analysis. The regression coefficients in the target relationship were determined by using multi regression analysis. The established relationship has been preliminarily applied for a set of large historical and instrumental earthquakes occurred along the DSFS. The established relationship has been globally estimated considering only three affecting variables. Therefore, it could be preliminary and applicable with some caution. Further efforts should be carried out to develop such an approach once more GPS Seismology data are available and additional affecting variables are included.

ACKNOWLEDGEMENTS

Authors would like to thank Prof. Khalil Ajami, President of the Syrian Virtual University (SVU) for his support of the scientific research. We are grateful to the two anonymous reviewers who presented suggestions and remarks for improving the manuscript. This manuscript benefited from helpful discussions with Profs. Muawia Barazangi (Cornell University), Francisco Gomez (University of Missouri) and Robert Reilinger (MIT). The GPS Seismology data have been processed using the software of the Cruncher Statistical System Company (Utah, USA).

REFERENCES

Abdul-Wahed M.K., Asfahani J., 2018, The recent instrumental seismicity of Syria and its implications. *Geof. Int.*, 57, 2, 121-138.

Abdul-Wahed M.K., Asfahani J., Al-Tahan I., 2011, A combined methodology of multiplet and composite focal mechanism techniques for the identification of the seismological active zones in Syria. *Acta Geophysica*, 59, 5, 967-992.

Abdul-Wahed M.K., Al-Tahan I., 2010, Preliminary outlining of the seismological active zones in Syria. *Annals of Geophysics*, 53, 4, 1-9.

Agnew D.C., Owen S., Shen Z. et al., 2002, Coseismic displacements from the Hector Mine, California, earthquake: results from survey-mode Global Positioning System measurements. *Bull. Seism. Soc. Am.*, 92, 1355-1364.

Altiner Y., Söhne W., Güney C. et al., 2013, A geodetic study of the 23 October 2011 Van, Turkey earthquake. Tectonophysics, 588, 118-134.

Ambikapathy A., Catherine J.K., Gahalaut V.K. et al., 2010, The 2007 Bengkulu earthquake, its rupture model and implications for seismic hazard. *J. Earth Syst. Sci.*, 119, 4, 553-560.

Ambraseys N.N., Melville C.P., 1988, An analysis of the eastern Mediterranean earthquake of 20 May 1202. Paper presented at the Symposium on History of Seismography and Earthquakes of the World, W.H. Lee (editor), (181-200). San Diego, California.

Ambraseys N.N., Barazangi M., 1989, The 1759 earthquake in the Bekaa Valley: implications for earthquake hazard assessment in the eastern Mediterranean region. *J. Geophys. Res.*, 94(B4), 4007-4013.

Ambraseys N.N., Finkel C.C., 1993, Material for the investigation of the seismicity of the Eastern Mediterranean region during the period 1690-1710. Paper presented at the Conference on Materials of the CEC Project: review of Historical Seismicity in Europe, M. Stucchi (ed.), (173-194), Milano: CNR.

Ambraseys N.N., Melville C.P., Adams R.D., 1994, The seismicity of Egypt, Arabia and the Red Sea: a historical review. King Abdulaziz City for Science and Technology and Cambridge University Press, 204 p.

Ambraseys N.N., Melville C.P., 1995, Historical evidence of faulting in eastern Anatolia and northern Syria. *Ann. Geophys.*, 38, 3-4, 337-343.

Anzidei M., Paldi P., Galvani A. et al., 1999, Coseismic displacement of the 27th September Umbria – Marche (Italy) earthquakes detected by GPS: campaigns and data. *Ann. Geophys.*, 42, 4, 597-607.

Arnadottir Th., Beavan J., Pearson Ch., 1995, Deformation associated with the 18 June 1994 Arthur' Pass earthquake, New Zealand. New Zealand *J. Geol. Geophys.*, 38, 4, 553-558.

Árnadóttir Th., Hreinsdóttir S., Gudmundsson G. et al., 2001, Crustal deformation measured by GPS in the south Iceland seismic zone due to two large earthquakes in June 2000. *Geophys. Res. Lett.*, 28, 21, 4031-4033.

Avallone A., Marzario M., Cerilla A. et al., 2011, Very high rate (10 Hz) GPS seismology for moderate-magnitude earthquakes: The case of the Mw 6.3 L'Aquila (central Italy) event. *J. Geophys. Res.*, 116., B02305. doi: 10.1029/2010JB007834.

Barnhart W.D., Murray J.R., Yun S.-H. et al., 2015, Geodetic constraints on the 2014 M 6.0 south Napa earthquake. *Seismol. Res. Lett.*, 86, 2A, 335-343.

Beavan J., Kendrick E., McCaffrey R. et al., 2006, Coseismic deformation of the May 2006 M 7.9 Tongo earthquake. American Geophysical Union, Fall Meeting, 2006. abstract id. T21F-04.

Beavan J., Samsonov S., Motagh M. et al., 2010, The Darfield (Canterbury) earthquake: Geodetic observations and preliminary source model. Bull. New Zealand Soc. *Earthq. Eng.*, 43, 4, 228-235.

Pizarro. M.B., Carrizo D., Socquet A., Armijo R., 2010, Asperities, Barriers and transition zone in the north Chile seismic gap: state of the art after the 2007 Mw 7.7 Tocopilla earthquake inferred by GPS and InSAR data. Paper presented at the Proc. "Fringe 2009 Workshop, Frascati, Italy.

Bekri E., Nankali H.R., Rahimi Z., 2015, Coseismic displacement of the earth crust using permanent GPS stations in Ahar-Varzeqan earthquake 2012. *Geosci. J.*, 24, 95, 105-110.

Bernard P., Briole P., Meyer B. et al., 1997, The Ms=6.2, June 15, 1995 Aigion earthquake (Greece): Evidence for low angle normal faulting in the Cornith rift. *J. Seismol.*, 1, 131-150.

Bilich A., Cassidy J.F, Larson C., 2008, GPS Seismology: application to the 2002 Mw 7.9 Denali fault earthquake. *Bull. Seism Soc. Am.*, 98, 2, 593-606.

Blewitt G., Heflin M.B., Hurst K.J. et al., 1993, Absolute far-field displacements from the 28 June 1992 Landers earthquake sequence. *Nature*, 361, 340-342.

Branzanti M., Colosimo G., Crespi M., Mazzoni A., 2013, GPS-near-real-time coseismic displacements for the great Tohoku-Oki earthquake. IEEE *Geosci. Remote S. Lett.*, 10, 2, 372-376.

Brockmann E., Hug R., Schneider D., Signer T., 2002, Geotectonics in the Swiss Alps using GPS. In Torres J.A. and H. Hornik (eds.), Subcommission for the European Reference Frame (UUREF), publication No. 11, 109-117.

Bürgmann R., Ayhan M.E., Fielding E.J. et al., 2002, Deformation during the 12 November 1999 Düzce, Turkey, earthquake, from GPS and InSAR data. *Bull. Seism. Soc. Am.*, 92, 1, 161-171.

Calais E., 2016, The Haiti 2010 earthquake.http://www.geologie.ens.fr/~ecalais/research/the-january-12th-2010-haiti/the-haiti-2010-earthquake.html.

Calais E., 2004, GPS campaign in the Dominican Republic, October 12-18, 2003: Data analysis and preliminary results. Technical Report. http://web.ics.purdue.edu /~ecalais/projects/caribbean/dr2003/

Calais E., Freed A., Mattioli G. et al., 2010, Transpressional rupture of an unmapped fault during the 2010 Haiti earthquake. *Nature Geosci. J.*, 3, 794-799.

Cheloni D., Serpelloni E., Devoti R. et al., 2016, GPS observations following the 2016, August 24, Mw 6 Amatrice earthquake (central Italy): Data, analysis and preliminary fault model. Ann. Geophys., 59, Fast Track 5.

Chen H.Y., L.Ch. Kuo L.Ch., Yu S., 2004, Coseismic movement and seismic ground motion associated with the 31 March 2002 off Hualien, Taiwan, earthquake. *Terr. Atmos. Ocean Sci.*, 15, 4, 683-695.

Chen H.Y., Yu S.B., Kuo L.C., Liu C.C., 2006, Coseismic and postseismic surface displacements of the 10 December 2003 (Mw 6.5) Chengkung, eastern Taiwan, earthquake. *Earth Planets Space*, 58, 5-21.

Chen H.Y., Lee J.C., Kuo L.C. et al., 2008, Coseismic surface GPS displacement and ground shaking associated with the 2006 Pingtung earthquake doublet, offshore southern Taiwan. *Terr. Atmos. Ocean Sci.*, 19, 6, 683-696.

Chen H.Y., Hsu Y.J., Lee J.Ch. et al., 2009, Coseismic displacements and slip distribution from GPS and leveling observations for the 2006 Peinan earthquake (Mw 6.1) in southeastern Taiwan. *Earth Planets Space*, 61, BF03352913.

Clarke P.J., Paradissis D., Briole P. et al., 1997, Geodetic investigation of the 13 May 1995 Kozani-Grevena (Greece) earthquake. *Geophys. Res. Lett.*, 24, 6, 707-710.

Darawcheh R., Abdul-Wahed M.K. and Hasan A., 2019, The 13th-August-1822 Aleppo earthquake: Implications for the seismic hazard assessment at the Antakia triple junction. N. Sundararajan et al. (eds.), Springer Nature Switzerland, 179-181.

De Chabalier J.B., Ruegg J.C., Armijo R. et al., 1997, Modelling the deformation related to the Mw = 8.1 subduction earthquake of northern Chile (1995) using SAR interferometry and GPS measurements. Eos, Transactions, AGU, Fall Meeting, F696.

Ding K., Freymueller J.T., Wang Q., Zou R., 2015, Coseismic and early postseismic deformation of the 5 January 2013 Mw 7.5 Craig earthquake from static and kinematic GPS solutions. *Bull. Seism. Soc. Am.*, 105(2B), 1153-1164.

Duputel Z., Jiang J., Jolivet R. et al., 2015, The Iquique earthquake sequence of April 2014: Bayesian modeling accounting for prediction uncertainty. *Geophys. Res. Lett.*, 42, 19, 7949-7957.

Ellis A.P., DeMets Ch., Briole P. et al., 2015, Geodetic slip solutions for the Mw = 7.4 Champerico (Guatemala) earthquake of 2012 November 7 and its postseismic deformation. *Geophys. J. Int.*, 201, 2, 856-868.

European Marine Observation and Data Network (EMODnet). http://www.emodnet.eu/

Fernandes R.M.S., Miranda J.M., Catalão J. et al., 2002, Coseismic displacements of the Mw = 6.1, July 9, 1998, Faial earthquake (Azores, north Atlantic). *Geophys. Res. Lett.*, 29, 16, 21-1 to 21-4.

Frontera T., Concha A., Blanco P. et al., 2012, DInSAR coseismic deformation of the May 2011 Mw 5.1 Lorca earthquake (southeastern Spain). *Solid Earth*, 3, 111-119.

Ganas A., Serpelloni E., Drakatos G. et al., 2009, The Mw 6.4 SW-Achaia (western Greece) earthquake of 8 June 2008: seismological, Field, GPS observations, and stress modeling. *J. Earthq. Eng.*, 13, 8, 1101-1124.

Ganas A., Cannavo F., Chousianitis K. et al., 2015, Displacements recorded on continuous GPS stations following the 2014 M6 Cephalonia (Greece) earthquakes: Dynamic characteristics and kinematic implications. *Acta Geodyn. Geomater.*, 12, 1, 5-27.

Ganas A., Elias P., Valkaniotis S., Briole P., 2017, Sentinel-1 reveals ground deformation after Aegean Sea earthquake. European Space Agency.

https://earth.esa.int/web/guest/content/-/article/sentinel-1-reveals-ground-deformation-after-aegean-sea-earthquake.

Geirsson H., Árnadóttir Th., Hiernsdóttir S. et al., 2010, Overview of results from continuous GPS observations in Iceland from 1995 to 2010. *Jökull*, 60, 3-22.

Geographical Survey Institute, GSI, 2003, Ground deformation in the 2003 Tokachi Oki earthquake. The 101st Meeting of the Coordinating Committee for Earthquake Prediction, Japan.

Giuliani R., Anzidei M., Bonci L. et al., 2007, Coseismic displacements associated to the Molise (southern Italy) earthquake sequence of October-November 2002 inferred from GPS measurements. *Tectonophysics*, 432, 1, 21-35.

Graham Sh.E., DeMets Ch., DeShon H.R. et al., 2012, GPS and seismic constraints on the M = 7.3 2009 Swan Islands earthquake: Implications for stress changes along the Motagua fault and other nearby faults. *Geophys. J. Int.*, 190, 3, 1625-1639.

Graham Sh.E., DeMets Ch., Cabral-Cano E. et al., 2014, GPS constraints on the Mw = 7.5 Ometepec earthquake sequence, southern Mexico: coseismic and post-seismic deformation. *Geophys. J. Int.*, 199, 200-218.

Group on Earth Observations, GEO (n.d.) Van, http://supersites.earthobservations.org/ van.php#GPS

Gunawan E., Kholil M., Meilano I., 2016, Splay-fault rupture during the 2014 Mw 7.1 Molucca Sea, Indonesia, earthquake determined from GPS measurements. *Phys. Earth Planet. In.*, 259, 29-33.

Hammond W.C., Blewitt G., Kreemer C. et al., 2011, Global Positioning System constraints on crustal deformation before and during the 21 February 2008 Wells, Nivada M6.0 earthquake. *Nivada Bureau of Mines and Geology*, Special Publication 36.

He P., Wang Q., Ding K., Li J., Zou R., 2016, Coseismic and postseismic slip ruptures for 2015 Mw 6.4 Pishan earthquake constrained by static GPS solutions. *Geod. Geodyn.*, 7, 5, 323-328.

Heflin M., n.d., GPS Time Series. https://sideshow.jpl.nasa.gov/post/series.html

Hill E.M., Borrero J.C., Huang Zh. et al., 2012, The 2010 Mw 7.8 Mentawai earthquake: Very shallow source of a rare tsunami earthquake determined from tsunami field survey and near-field GPS data. *J. Geophys. Res.*, 117, B6. doi:10.1029/2012JB009159.

Hoechner A., Babeko A.Y., Sobolev S.V., 2008, Enhanced GPS inversion technique applied to the 2004 Sumatra earthquake and tsunami. *Geophys. Res. Lett.*, 35, 8, L08310.

Hollenstein Ch., Müller M.D., Geiger A., Kahle H.G., 2008, GPS-derived coseismic displacements associated with the 2001 Skyros and 2003 Lefkada earthquakes in Greece. *Bull. Seismol. Soc. Am.*, 98, 1, 149-161.

Houlié N., Dreger D., Kim A., 2014, GPS source solution of the 2004 Parkfield earthquake. *Sci. Rep.*, 4, 3646. doi: 10.1038/srep03646.

Hsu Y.J., Yu Sh.B., Kuo L.Ch. et al., 2011, Coseismic deformation of the 2010 Jiashian, Taiwan earthquake and implications for fault activities in southwestern Taiwan. *Tectonophysics*, 502, 328-335.

Hudnut K., Shen Z., Murray M., et al., 1996, Co-seismic displacements of the 1994 Northridge, California, earthquake. *Bull. Seism. Soc. Am.*, 86, 1B, S19-S36.

Hung J.H., Zhan H.P., Wiltschko D.V., Fang P., 2002, Geodetically observed surface displacements of the 1999 Chi-Chi earthquake near southern termination of the Chelungpu fault. *Terr. Atmos. Ocean Sci.*, 13, 3, 355-366.

Hutton W., DeMets C., Sánchez O. et al., 2001, Slip kinematics and dynamics during and after the 1995 October 9 Mw 8.0 Colima-Jalisco earthquake, Mexico, from GPS geodetic constraints. *Geophys. J. Int.*, 146, 3, 637-658.

INGV Working Group, 2016, Preliminary co-seismic displacements for the October 26 (Mw 5.9) and October 30 (Mw 6,5) central Italy earthquakes from the analysis of GPS stations. doi: 10.5281/zenodo/167959. http://ring.gm.ingv.it/?p=1304.

International Seismological Center, ISC, On-line ISC Bulletin. http://www.isc.ac.

Ito T., Gunawan E., Kimata F. et al., 2016, Co-seismic offsets due to two earthquakes (Mw 6.1) along the Sumatran fault system derived from GNSS measurements. Earth Planets Space, 68, 57. https://doi.org/10.1186/s40623-016-0427-z.

Jade S., Mukul M., Parvez I.A. et al., 2003, Pre-seismic, co-seismic and post-seismic displacements associated with the Bhuj 2001 earthquake derived from recent and historical geodetic data. *J. Earth Syst. Sci.*, 112, 3, 331-345.

Kaiser A., Holden C., Beavan J. et al., 2012, The Mw 6.2 Christchurch earthquake of February 2012: Preliminary report. New Zealand J. Geol., 55, 1, 67-90.

Kimata F., Tealeb A., Murakami H. et al., 1997, The Aqaba earthquake of November 22, 1995 and co-seismic deformation in Sinai Peninsula deduced from repeated GPS measurements. *Acta Geod. Geophys*. Hu., 32, 1-2, 53-71.

Klein E., Vigny Ch., Fleitout L. et al., 2017, A comprehensive analysis of the Illapel 2015 Mw 8.3 earthquake from GPS and InSAR data. *Earth Planet. Sci. Lett*., 468, 123-134.

Kreemer C., Blewitt G., Maerten F., 2006, Co- and postseismic deformation of the 28 March 2005 Nias Mw 8.7 earthquake from continuous GPS data. Geophys. Res. Lett., 33, L07307. doi: 10.1029/2005GL05566.

Kutoglu H.S., Celik R.N., Ozludemir M.T., Güney C., 2011, New findings on the effects of the İzmit Mw=7.4 and Düzce Mw=7.2 earthquakes. *Nat. Haz. Earth Syst. Sci*., 11, 267-272.

Larson K.M., 2009, GPS Seismology. *J. Geod.*, 83, 3-4, 227-233. doi:10.1007/s00190-008-0233-x.

Lai K.-Yuang, Chen Y.-Gau, Wu Y.-Min et al. ,2009, The 2005 Ilan earthquake doublet and seismic crisis in northwestern Taiwan: Evidence for dyke intrusion associated with on-land propagation of the Okinawa trough. *Geophys. J. Int.*, 179, 2, 678-686.

Lundgren P.R., Wolf S.K., Protti M., Hurst K.J., 1993, GPS measurements of crustal deformation associated with the Valle da la Estrella, Costa Rica earthquake. *Geophys. Res. Lett.*, 20, 5, 407-410.

Mahesh P., Kundu B., Katherine J.K., Gahalaut V.K., 2011, Anatomy of the 2009 Fiordland earthquake (Mw 7.8), South Island, New Zealand. *Geosci. Front.*, 2, 1, 17-22.

Meng G., Ren J., Su X. et al., 2013, Coseismic deformation of the 2010 Mw 6.9 Yushu earthquake derived from GPS data. Seismol. Res. Lett., 84, 1, 57-64.

Min-Chien T., Chi-Yu Ch., Shuo-Ying W. and IES GPS Team, 2013, GPS coseismic displacements distribution of Ruisui earthquake at 31 Oct. 2013, Taiwan. http://tec.earth.sinica.edu.tw/new_web/upload/news/Conference/20131031RuisuiEQ/06_Tsai%20Min-Chien.pdf.

Nakao Sh., Yakiwara H., Hirano Sh. et al., 2016, Crustal deformation by the West Off Satsuma Peninsula earthquake occurred on November 14, 2015. *Japan Geoscience Union Meeting*, 22-26 May 2016, Tokyo.

NCSS 11 Statistical Software, 2016), NCSS, LLC. Kaysville, Utah, USA, ncss.com/software/ncss.

Nevada Geodetic laboratory, NGL, n.d., Latest News. http://geodesy.unr.edu/ and https://www.unavco.org/highlights/2014/ferndale.html

Nishimura T., Fujiwara S., Murakami M. et al., 2006, Fault model of the 2005 Fukuoka-ken Seiho-oki earthquake estimated from coseismic deformation observed by GPS and InSAR. *Earth Planets Space*, 58, 51-56.

Nishimura T., Hashimoto M., Hoso Y. et al., 2017, Crustal deformation of the 2016 October 21th M 6.6 earthquake in central Tottori Prefecture. JpGU-AGU Joint Meeting 2017, Tokyo.

Nocquet J.-M., Jarrin P., Vallée M. et al., 2017, Supercycle at the Ecuadorian subduction zone revealed after the 2016 Pedernales earthquake. Nat. Geosci., 10, 145-149.

Nykolaishen L., Dragert H., Wang K. et al., 2015, GPS observations of crustal deformation associated with the 2012 Mw 7.8 Haida Gwaii earthquake. *Bull. Seism. Soc. Am.*, 105, 2B, 1241-1252.

Ohta Y., Miura S., Ohzono M. et al., 2011, Large intraslab earthquake (2011 April 7, M 7.1) after the 2011 off the Pacific coast of Tohoku earthquake (M 9.0): Coseismic fault model based on the dense GPS network data. *Earth Planets Space*, 63, 1207-1211.

O'Keefe K., Fortes L.P., 2001, Using permanent GPS stations to detect the 2001 Nisqually earthquake. Proceedings of the Scientific Assembly of the International Association of Geodesy (Paper 170BD, 5 pages), Budapest, Hungary.

Ozawa Sh., Yarai H., Tobita M. et al., 2008, Crustal deformation associated with the Noto Hanto earthquake in 2007 in Japan. *Earth Planets Space*, 60, 95-98.

Polcari M., Albano M., Fernández J. et al., 2016, Three-dimensional (3D) coseismic deformation map produced by the 2014 south Napa earthquake estimated and modeled by SAR and GPS data integration. European Geosciences Union General Assembly (EGU), Vienna, Austria, p. 12959.

Pollitz F.F., Wicks Ch., Schoenball M. et al., 2017, Geodetic slip model of the 3 September 2016 Mw 5.8 Pawnee, Oklahoma, earthquake: evidence for fault-zone collapse. *Seismol. Res. Lett.*, 88, 4, 983-993.

Pradhan R., Prajapati S.K., Chopra S. et al., 2013, Causative source of Mw 6.9 Sikkim-Nipal border earthquake of September 2011: GPS baseline observations and strain analysis. *J. Asian Earth Sci.*, 70-71, 179-192.

Pritchard M.E., Norabuena E.O., Ji C. et al., 2007, Geodetic, teleseismic, and strong motion constraints on slip from recent southern Peru subduction zone earthquakes. *J. Geophys. Res.*, 112 (B03307).

Protti M., González V., Newman A.V. et al., 2014, Nicoya earthquake rupture anticipated by geodetic measurement of the locked plate interface. *Nat. Geosci.*, 7, 117-121.

Regnier M., Calmant S., Pelletier B. et al., 2003, The Mw 7.5 1999 Ambrym, Vanuatu: a pack arc intraplate thrust event. *Tectonics*, 22, 4, 1043.

Reigber Ch., Xia Y., Michel G.W. et al., 1997, The Antofagasta 1995 earthquake: Crustal deformation pattern as observed by GPS and D-INSAR. The 3rd ERS Symposium, Florence.

Ruddick R., 2005, Analysis of the 2002 Mw = 7.6 Wewak earthquake, Papua New Guinea, using Global Positioning System observations. Thesis of Honours, The Australian National University, Canberra, 91 p.

Ruiz S., Klein E., del Campo F. et al., 2016, The seismic sequence of the 16 September 2015 Illapel Mw 8.3 earthquake. Seismol. Res. Lett., 87, 4, 789-799.

Savage J.C., Burford R.O., 1973, Geodetic determination of relative plate motion in central California. *J. Geophys. Res.*, 78, 5, 832-845.

Sbeinati M. R., Darawcheh R., Mouti M., 2005, The historical earthquakes of Syria: An analysis of large and moderate earthquakes from 1365 B.C. to 1900 A.D. *Ann. Geophys.*, 48, 3, 347-435.

Schmitt S.V., DeMets Ch., Stock J. et al., 2007, A geodetic study of the 2003 January Tecomán, Colima, Mexico earthquake. *Geophys. Res. Int.*, 169, 2, 389-406.

School of Ocean and Earth Science and Technology, SOEST, 2015, Preliminary coseismic displacement field M8.8 Maule earthquake, Chili, Feb 27, 2010. University of Hawai' I at Mãnoa.

Scordilis E.M., 2006, Empirical global relations converting Ms and mb to moment magnitude. *J. Seismol.*, 10, 225-236. doi: 10.1007/s10950-006-9012-4.

Seeüller W., Kaniuth K., Drewes H., 2001, Velocity estimates of IGS RNAAC SIRGAS stations. International Association of Geodesy Symposium, Cartagena, Colombia.

Serpelloni E., Anderlini L., Avallone A. et al., 2012, GPS observations of coseismic deformation following the May 20 and 29, 2012, Emilia seismic events (northern Italy): Data, analysis and preliminary models. *Ann. Geophys.*, 55, 4, 759-766.

Shao G., Ji C., Zhao D., 2011, Rupture process of the 9 March, 2011 Mw 7.4 Sanriku-Oki, Japan earthquake constrained by jointly inverting teleseismic waveforms, strong motion data and GPS observations. *Geophys. Res. Lett.*, 38, L00G20.

Smith-Konter B., Sandwell D., Shearer P., 2011, Locking depths estimated from geodesy and seismology along the San Andreas Fault System: Implications for seismic moment release. *J. Geophys. Res.*, 116, B06401.

Som S.K., Jana P., Mohapatra S.R. et al., 2013, Mw 5.9, 18th June 2010 earthquake and fault segment linkage at Andaman - a study based on macroseismic survey, GPS Geodesy and Coulomb stress changes. *J. Asian Earth Sci.*, 67, 26-36.

Stanaway R., 2008, Papua New Guinea on the move-GPS monitoring of plate tectonics and earthquakes. The 42nd Association of Surveyors PNG Congress, Port Moresby.

Stein R.S., Marshall G.A., Murray M.H. et al., 1993, Permanent ground movement associated with the 1992 M=7 Cape Mendocino, California, earthquake: Implications for damage to infrastructure and hazard to navigation. *U.S. Geological Survey*, Open-File Report 93-383.

Tabei T., Kato T., Catane J.P.L. et al., 1996, Crustal deformation associated with the 1995 Hyogo-ken Nanbu earthquake, Japan derived from GPS measurements. *Phys. Earth Planet Int.*, 44, 281-286.

Tahayt A., Feigl K.L., Mourabit T. et al., 2009, The Al-Hoceimah (Morocco) earthquake of 24 February 2004, analysis and interpretation of data from ENVISAT ASAR and SPOT5 validated by ground-based observation. *Remote Sens. Environ.*, 113, 306-316.

Al-Tarazi E., 2000, The major gulf of the Aqaba earthquake, 22 November 1995-maximum intensity distribution. *Nat. Haz.*, 22, 17-27.

Al-Tarazi E., Abu Rajab J., Gomez F. et al., 2011, GPS measurements of the near-field deformation along the southern Dead Sea fault system. Geochem. *Geophys. Geosystems*, 12, 12, Q12021. doi:10.1029/2011GC003736.

Terry R.L., Funning G.J., Floyd M., 2017, A study of the December 2016, The Geysers, CA earthquake using InSAR and GPS. Poster presented at 2017 Southern California Earthquake Center Annual Meeting. University of Southern California, Los Angeles.

Timofeev V.Y., Ardyukov D.G., Stus Y.F. et al., 2008, Pre-, co and post-seismic motion for the Altay region by GPS and gravity observations. The International Conference ETS, Weimar, Germany, 11687-11705.

Tsai M.C., Shin T.C., Kuo K.W., 2017, Pre-seismic strain anomalies and coseismic deformation of the Meinong earthquake from continuous GPS. Terr. Atmos. Ocean Sci., 28, 5. doi: 10.3319/TAO.2017.04.19.01.

Tyriakioğlu I., 2015, Geodetic aspects of the 19 May 2011 Simav earthquake in Turkey. Geomatics, *Nat. Haz. Risk*, 6, 1, 76-89.

UNAVCO, 2010, Gorda earthquake recorded in PBO GPS 15-second time series. https://www.unavco.org/highlights/2010/gorda-earthquake-recorded-in-pbo-gps-15-second-time-series.html

United States Geological Survey, USGS, Homepage, http://www.usgs.gov

Wang K., Fialko Y., 2015, Slip model of the 2015 Mw 7.8 Gorkha (Nepal) earthquake from inversions of ALOS-2 and GPS data. *Geophys. Res. Lett.*, 42, 18,, 7452-7458.

Wang M., Wan Y., Shen Zh. et al., 2006, Coseismic slip distribution of the 2001 Kokoxili, northern Tibet, earthquake, constrained by GPS and geological field survey data. Tectonophysics.

Weber J.C., Geirsson H., Latchman J.L. et al., 2015, Tectonic inversion in the Caribbean-south American plate boundary: GPS geodesy, seismology, and tectonics of the Mw 6.7 22 April 1997 Tobago earthquake. *Tectonics*, 34, 1181-1194.

Wells D.L., Coppersmith K.J., 1994, New empirical relationships among magnitude, rupture length, rupture width, rupture area, and surface displacement. *Bull. Seism. Soc. Am.*, 84, 4, 974-1002.

Williams C.R., Segall P., 1996, Coseismic displacements measured by Global Positioning System. In Paul Spidich (ed.), The Loma Prieta, California, Earthquake of October 17, 1989-Main shock characteristics (236-278), Washington.

Wiseman K., Banerjee P., Bürgmann R. et al., 2012, Source model of the 2009 Mw 7.6 Padang intraslab earthquake and its effect on the Sunda megathrust. *Geophys. J. Int.*, 190, 1710-1722.

Yamazaki F., Moya L., Anekoji K., Liu W., 2014, Comparison of the coseismic displacements obtained from strong motion accelorograms and GPS data in Japan. *Second European Conference on Earthquake Engineering and Seismology*, Istanbul.

Yarai H., Kobayashi T., Morishita Y. et al., 2016, Crustal deformation of the 2016 Kumamoto earthquake. *Japan Geoscience Union Meeting*, Tokyo.

Yelles K., Lammali K., Mahsas A. et al., 2004, Coseismic deformation of the May 21st, 2003, Mw=6.8 Boumerdes earthquake, Algeria, from GPS measurements. *Geophys. Res. Lett.*, 31, 13, L13610. doi: 10.1029/2004GL019884.

Yiğit C. Ö, Tiryakioğlo I., Saka M.H., Alkan R.M., 2015, GNSS-derived coseismic displacement of the Gökçeada earthquake (2014, Mw:6.9) based on 1 Hz GNSS data. *Geophys. Res. Abstr.*, 17, EGU2015, EGU General Assembly.

Yin H., Wdowinski Sh., Liu X. et al., 2013, Strong ground motion recorded by high-rate GPS of the 2008 Ms 8.0 Wenchuan earthquake, China. *Seismol. Res. Lett.*, 84, 2, 210-218.

Yokota Y., Koketsu K., Hikima K., Miyazaki Sh., 2009, Ability of 1-Hz GPS data to infer the source process of a medium-sized earthquake: The case of the 2008 Iwate-Miyagi Nairiku, Japan. *Geophys. Res. Lett.*, 36, L12301.

Yong H., Shaomin Y., Bin Zh. et al., 2013, The coseismic displacements of the 2013 Lushan Mw 6.6 earthquake determined using continuous global positioning system measurements. *Geod. Geodyn.*, 4, 2, 6-10.

Yongge W., Zhengkang Sh., Zhende H. et al., 2005, Co-seismic slip distribution of the 2001 Kokoxili earthquake inverted by GPS data. *Earthq. Res. China*, 19, 4, 420-429.

Zheng Y., Li J., Xie Z., Ritzwoller M.H., 2012, 5Hz GPS seismology of the El Mayor-Cucapah earthquake: estimating the earthquake focal mechanism. *Geophys. J. Int.*, 190, 1723-1732.

Zohar M., Marco Sh., 2012, Re-estimating the epicenter of the 1927 Jericho earthquake using spatial distribution of intensity data. *J. Appl. Geophys.*, 82, 19-29.

Appendix 1: List of 120 interplate worldwide earthquakes measured by near-field GPS stations.

#	Date (mm/dd/yy)	Earthquake/Location	Faulting type	M_w	h (km)	GPS Site (ID)	Δ (km)	D_{GPS} (cm)	Reference(s)
1	10/17/1989	Loma Prieta/US	R	6.9	19	TRAILL*	12	41.30	Williams and Segall, 1996
2	04/22/1991	Limon/CR	T	7.7	10	LIMO*	50	244.7	Lundgren *et al.*, 1993
3	04/24/1992	Mendocino/US	T	7.1	11	Pierce E.	13	40	Stein *et al.*, 1993
4	06/28/1992	Landers/US	R	7.3	07	DEAD	30	53.7	Blewitt *et al.*, 1993
5	01/17/1994	Northridge/US	T	6.7	18	SAFE*	10	21.6	Hudnut *et al.*, 1996
6	06/18/1994	Arthur' Pass/NZ	T	6.7	15	-*	10	50	Arnadottir *et al.*, 1995
7	01/17/1995	Kobe/JP	R	7.2	17	IWAY*	5	45	Tabei *et al.*, 1996
8	05/13/1995	Kozani/GR	N	6.6	14	-*	10	20	Clarke *et al.*, 1997
9	06/15/1995	Aigion/GR	N	6.4	10	C075*	0	7	Bernard *et al.*, 1997
10	07/30/1995	Antofagasta/CL	T	8.1	36	DO3*	25	100	De Chabalier *et al.*, 1997; Reigber *et al.*, 1997
11	10/09/1995	Colima/MX	T	8.0	40	CHAM*	50	90	Hutton *et al.*, 2001
12	11/22/1995	Nuweiba/Gulf of Aqaba	L+N	7.0	13	DHAB*	26	17	Kimata *et al.*, 1997
13	11/12/1996	Nazca/PE	T	7.7	33	ZAMA*	50	13.45	Pritchard *et al.*, 2007
14	04/22/1997	Tobago/TT	N	6.7	09	FTMD*	12.5	14.3	Weber *et al.*, 2015
15	09/26/1997	Umbria/IT	N	6.0	06	CROC*	< 2	14	Anzidei *et al.*, 1999
16	07/09/1998	Faial/Azores	R+L	6.1	05	FAIM*	20	5.9	Fernandes *et al.*, 2002
17	07/17/1998	Rayli/TW	T	6.2	03	S326*	5	2.3	Hung *et al.*, 2002
18	08/17/1999	İzmit/TR	R	7.4	15	G240026*	60	200	Kutoglu *et al.*, 2011
19	09/21/1999	Chi Chi/TW	T+L	7.5	08	I007	10	132	Hung *et al.*, 2002
20	10/16/1999	Hector Mine/US	S	7.1	20	-*	< 3	100	Agnew *et al.*, 2002
21	11/12/1999	Düzce/TR	R	7.2	14	MUDR*	40	12	Bürgmann *et al.*, 2002
22	11/26/1999	Ambrym/VU	T	7.5	14	AMBR	50	35	Regnier *et al.*, 2003
23	06/17/2000	IS	R	6.5	06	-*	2.5	28	Árnadóttir *et al.*, 2001
24	06/21/2000	IS	R	6.4	06	-*	5	27	Árnadóttir *et al.*, 2001
25	11/16/2000	New Ireland/GY	T	8.0	33	RVO	33	59	Stanaway, 2008
26	01/13/2001	Coast/SV	N	6.5	10	SSIA	20	0.7	Seeüller *et al.*, 2001
27	01/26/2001	Bhuj/IN	T	7.6	16	KAKA	20	100	Jade *et al.*, 2003
28	02/13/2001	San Salvador/SV	L	6.6	10	SSIA	25	4.3	Seeüller *et al.*, 2001
29	02/28/2001	Nisqually/US	N	6.8	59	RPTI	30	1	O'Keefe and Fortes, 2001
30	06/23/2001	Arequipa/PE	T	8.5	32	JHAI	70	107	Pritchard *et al.*, 2007
31	07/17/2001	Lana/IT	-	4.8	-	BZRG	10	2.7	Brockmann *et al.*, 2002
32	07/26/2001	Skyros/GR	L	6.4	12	DUKA	30	7	Hollenstein *et al.*, 2008
33	11/14/2001	Kokoxili/Tibet	L	7.9	15	BS33	10	80	Yongge *et al.*, 2005; Wang *et al.*, 2006
34	03/31/2002	331/TW	-	7.0	10	SAUO	50	5.5	Chen *et al.*, 2004
35	09/08/2002	Wewak/PG	T	7.6	13	XAVI	20	121	Ruddick, 2005

36	10/31/2002	Molise/IT	R	5.7	20	CROC	4	2.4	Giuliani *et al.*, 2007
37	11/03/2002	Denali Fault/Alaska	R	7.9	05	WHIT	~ 10	50	Larson, 2009; Bilich *et al.*, 2008
38	01/22/2003	Tecomán/MX	T	7.2	24	COLI	~70	15	Schmitt *et al.*, 2007
39	05/21/2003	Boumerdes/DZ	T	6.8	10	BOUB*****	20	25	Yelles *et al.*, 2004
40	08/14/2003	Lefkada/GR	R	6.2	15	-	30	7.2	Hollenstein *et al.*, 2008
41	09/22/2003	Puerto Plata/DO	T	6.5	-	REUN	10	7.8	Calais, 2004
42	09/26/2003	Tokachi-oki/JP	T	8.0	27	0532	70	100	Larson, 2009; GSI, 2003
43	09/27/2003	Chuya/Altay	R	7.3	-	KURA*****	15	35	Timofeev *et al.*, 2008
44	12/10/2003	Chengkung/TW	T	6.5	18	CHEN	5	13	Chen *et al.*, 2006
45	12/22/2003	San Simeon/US	T	6.5	16	CRBT	35	10	Larson, 2009
46	02/24/2004	Al Hoceima/MA	L	6.3	12	BBFH	30	3	Tahayt *et al.*, 2009
47	09/28/2004	Parkfield/US	S	6.0	08	HUNT	25	4.9	Houlié *et al.*, 2014
48	12/26/2004	Sumatra/ID	T	9.2	30	-	80	500	Hoechner *et al.*, 2008
49	03/05/2005	Ilan/TW	N	5.7	07	LTUN	5	3	Lai *et al.*, 2009
50	03/20/2005	Fukuoka-ken/JP	L	6.6	09	021062	15	20	Nishimura *et al.*, 2006
51	03/28/2005	Nias/ID	T	8.7	30	LHWA	30	500	Kreemer *et al.*, 2006
52	04/01/2006	Peinan/TW	L?	6.1	11	LONT	5	4.5	Chen *et al.*, 2009
53	05/05/2006	Tonga/NZ	T	7.9	15	-	90	40	Beavan *et al.*, 2006
54	12/26/2006	Pingtung/TW	N	7.0	44	HENC	40	3.5	Chen *et al.*, 2008
55	12/26/2006	Pingtung/TW	-	6.9	33	HENC	40	3.2	Chen *et al.*, 2008
56	03/25/2007	Noto Hanto/JP	T	6.9	11	0575	10	21	Ozawa *et al.*, 2008
57	07/16/2007	Chuetsu-Niigata/JP	T	6.5	10	0051	25	80	Larson, 2009
58	09/12/2007	Bengkulu/ID	T	8.4	30	LIAS	90	73	Ambikapathy *et al.*, 2010
59	11/14/2007	Tocopilla/CL	T	7.7	40	BMEJ	50	30	Pizarro *et al.*, 2010
60	02/21/2008	Wells/US	N	6.0	-	GOSH	80	0.15	Hammond *et al.*, 2011
61	05/12/2008	Sichauan/CN	T	7.9	15	PIXI-51	38	40	Yin *et al.*, 2013
62	05/29/2008	-/IS	R+N	6.3	10	BALD	30	20	Geirsson *et al.*, 2010
63	06/08/2008	Achaia/GR	S	6.4	18	RLS	12.8	0.73	Ganas *et al.*, 2009
64	06/14/2008	Iwate-Miyagi/JP	T	6.9	08	0928	20	20	Yokota *et al.*, 2009
65	04/06/2009	Aquila/IT	N	6.3	10	ROIO	2.3	8.5	Avallone *et al.*, 2011
66	05/28/2009	Swan Islands/HN	-	7.3	10	ROA0*****	50	31	Graham *et al.*, 2012
67	07/15/2009	Fiordland/NZ	T	7.8	12	PYGR	30	30	Mahesh *et al.*, 2011
68	09/30/2009	Padang/ID	T	7.6	80	MSAI	35	5	Wiseman *et al.*, 2012
69	01/10/2010	Gorda/US	-	6.5	22	P162	30	25	UNAVCO, 2010
70	01/12/2010	HT	-	7.0	13	DFRT	5	80	Calais, 2016; Calais *et al.*, 2010
71	02/27/2010	Maule/CL	T	8.8	35	CONZ	70	300	SOEST, 2015
72	03/04/2010	Jiashian/TW	T	6.4	23	GS51	25	2.7	Hsu *et al.*, 2011
73	04/04/2010	El Mayor-Cucapah/MX	-	7.2	10	P496	62	78	Zheng *et al.*, 2012
74	04/13/2010	Yushu/CN	-	6.9	10	JB94	10	1.5	Meng *et al.*, 2013
75	06/18/2010	Andaman/Bengal B.	-	5.9	20	ABAY*****	2	11	Som *et al.*, 2013
76	09/04/2010	Darfield/NZ	-	7.1	10	MQZG	30	14	Beavan *et al.*, 2010
77	10/25/2010	Mentawai/ID	T	7.8	20	BSAT	49	22	Hill *et al.*, 2012
78	02/22/2011	Christchurch/NZ	-	6.2	05	-	2	30	Kaiser *et al.*, 2012
79	03/09/2011	Sanriku-oki/JP	-	7.4	08	-	80	3.2	Shao *et al.*, 2011
80	03/11/2011	Tohaku-oki/JP	T	9.0	06	MIZU	140	240	Branzanti *et al.*, 2013
81	04/07/2011	NE of Japan	T	7.1	66	KNK	50	3	Ohta *et al.*, 2011
82	04/11/2011	Fukushima/JP	-	6.6	06	0800	20	28	Yamazaki *et al.*, 2014
83	05/11/2011	Lorca/ES	T	5.1	02	LORC	5	0.6	Frontera *et al.*, 2012
84	05/19/2011	Simav/TR	N	5.9	09	DEIR	10	0.2	Tyriakioğlu, 2015
85	09/18/2011	Sikkim-Nepal	-	6.9	20	PHOD	40	2	Pradhan *et al.*, 2013
86	10/23/2011	Van/TR	T	7.2	07	MURA	43	3.8	Altiner *et al.*, 2013; GEO, n.d
87	03/20/2012	Ometepec/MX	T	7.5	15	OMTP	50	28	Graham *et al.*, 2014
88	05/20/2012	Emilia/IT	T	6.1	10	MO05	< 5	3	Serpelloni *et al.*, 2012

89	05/29/2012	Emilia/IT	T	5.8	05	CONC	< 5	1	Serpelloni *et al.*, 2012
90	08/11/2012	Ahar-Varzeqan/AZ	-	6.0	10	-	20	0.5	Bekri *et al.*, 2015
91	09/05/2012	Nicoya/CR	T	7.6	40	-	40	68	Protti *et al.*, 2014
92	10/28/2012	Haida Gwaii/CA	T	7.8	18	BARI	30	115	Nykolaishen *et al.*, 2015
93	11/07/2012	Champerico/GT	T	7.4	24	-	65	6	Ellis *et al.*, 2015
94	01/05/2013	Craig/Alaska	T	7.5	10	AB48	114	12	Ding *et al.*, 2015
95	01/21/2013	Sumatra/ID	-	6.1	10	GEUM	< 10	7.4	Ito *et al.*, 2016
96	04/20/2013	Lushan/CN	T	6.6	22	SCTQ	43.3	3	Yong *et al.*, 2013
97	07/02/2013	Sumatra/ID	-	6.1	10	CELA	2	4.5	Ito *et al.*, 2016
98	10/31/2013	Ruisui/TW	-	6.3	19	JPEI	2	5	Min-Chien *et al.*, 2013
99	01/26/2014	Cephalonia/GR	-	6.0	16	VLSM	11	3.35	Ganas *et al.*, 2015
100	02/03/2014	Cephalonia/GR	-	5.9	05	VLSM	11	7	Ganas *et al.*, 2015
101	03/09/2014	Ferndale/US	-	6.8	16	P162	90	1.5	NGL, n.d.
102	04/01/2014	Iquique/CL	T	8.1	20	PSGA	80	100	Duputel *et al.*, 2015
103	05/24/2014	Gökçeada/Aegean Sea	-	6.9	10	-	90	11	Yiğit *et al.*, 2015
104	08/24/2014	South Napa/US	-	6.0	11	-	5	15	Polcari *et al.*, 2016; Barnhart *et al.*, 2015
105	11/15/2014	Molucca Sea/ID	-	7.1	35	CTER	100	1.5	Gunawan *et al.*, 2016
106	04/25/2015	Gorkha/NP	T	7.8	08	-	50	150	Wang and Fialko, 2015
107	07/03/2015	Pishan/CN	T	6.4	15	A506*****	17.5	12	He *et al.*, 2016
108	09/16/2015	Illapel/CL	T	8.3	22	BFRJ	40	200	Klein *et al.*, 2017; Ruiz *et al.*, 2016
109	11/14/2015	Southern coast/JP	-	7.0	10	UJIS	84	1.32	Nakao *et al.*, 2016
110	02/06/2016	Meinong/TW	SS+TF	6.4	15	NEMN	11	5	Tsai *et al.*, 2017
111	04/16/2016	Pedernales/EC	T	7.8	21	-	50	40	Nocquet *et al.*, 2017
112	04/16/2016	Kumamoto/JP	R	7.3	10	0701	10	97	Yarai *et al.*, 2016
113	08/24/2016	Amatrice/IT	N	6.0	08	AMAT	10	3	Cheloni *et al.*, 2016
114	09/03/2016	Pawnee/US	-	5.8	05	OKPR	40	0.1	Pollitz *et al.*, 2017
115	10/21/2016	Tottori/JP	-	6.6	-	KRNS	5	9	Nishimura *et al.*, 2017
116	10/26/2016	Macerata/IT	-	5.9	10	FIAB	10	3.1	INGV Working Group, 2016
117	10/30/2016	Vittore/IT	N	6.5	10	VITT	10	38.3	INGV Working Group, 2016
118	11/13/2016	Kaikora/NZ	T	7.8	15	CMBL	50	26.4	NGL, n.d.
119	12/14/2016	The Geysers/US	-	5.0	02	-	10	1	Terry *et al.*, 2017
120	07/20/2017	Aegean Sea/Med. Sea	N	6.6	10	-	70	1	Ganas *et al.*, 2017

Notes

- Names of the countries (column 3) are given by their shortcuts as follows: AZ: Azerbaijan; CA: Canada; CH: Switzerland; CL: Chile; CN: China; CR: Costa Rica; DO: Dominican Republic; DZ: Algeria; EC: Ecuador; ES: Spain; GR: Greece; GT: Guatemala; GY: Guyana; HN: Honduras; HT: Haiti; ID: Indonesia; IN: India; IS: Iceland; IT: Italy; JP: Japan; MA: Morocco; MX: Mexico; NP: Nepal; NZ: New Zealand; PE: Peru; PG: Papua New Guinea; SV: El Salvador; TR: Turkey; TW: Taiwan; US: United States of America,; VU: Vanuatu.
- Fault mechanisms (column 4): N = normal fault; L = left-lateral strike-slip; R = right-lateral strike-slip; T = thrust, with a combination of these symbols for oblique motions. Some mechanisms were taken from other references not mentioned in column 9.
- Mw (column 5): Some M_s values are converted to M_w using the relationship developed by Scordilis (2006).
- h (column 6) is the focal depth of the earthquake.
- GPS site (column 7): ***** indicates the survey-mode GPS (sGPS) measurements; - = no station mentioned in the paper.
- Δ (column 8) denotes the distance between the epicenter of the earthquake and the nearest GPS site.
- D_{GPS} (column 9) is a horizontal coseismic displacement.